Title: Spatial variation in exploited metapopulations obscures risk of collapse

Authors: Daniel K Okamoto[a,b,c*], Margot Hessing-Lewis[b], Jameal F Samhouri[d], Andrew O Shelton[d], Adrian Stier[e], Philip S Levin[f,g] and Anne K Salomon[b,c]

a: Department of Biological Science, Florida State University

b: Hakai Institute

c: School of Resource and Environmental Management, Simon Fraser University

d: Conservation Biology Division, Northwest Fisheries Science Center, National Marine Fisheries Service, National Oceanic and Atmospheric Administration

e: Department of Ecology, Evolution, and Marine Biology, University of California, Santa Barbara

f: The Nature Conservancy

g: School of Environment and Forestry Sciences, University of Washington

*corresponding author: dokamoto@bio.fsu.edu

Running Head: Cryptic collapses in metapopulations

Author contributions:

DKO designed, built and conducted analyses. AS conducted the home-range literature review. DKO and AKS wrote the initial manuscript draft. DKO, MHL, JFS, AOS, AS, PSL, and AKS initiated the research focus, refined analyses and contributed to revisions.

Abstract

Unanticipated declines among exploited species have commonly occurred despite harvests that appeared sustainable prior to collapse. This is particularly true in the oceans where spatial scales of management are often mismatched with spatially complex metapopulations. We explore causes, consequences and potential solutions for spatial mismatches in harvested metapopulations in three ways. First, we generate novel theory illustrating when and how harvesting metapopulations increases spatial variability and in turn masks local scale volatility. Second, we illustrate why spatial variability in harvested metapopulations leads to negative consequences using an empirical example of a Pacific herring metapopulation. Finally, we construct a numerical management strategy evaluation model to identify and highlight potential solutions for mismatches in spatial scale and spatial variability. Our results highlight that spatial complexity can promote stability at large scales, however ignoring spatial complexity produces cryptic and negative consequences for people and animals that interact with resources at small scales. Harvesting metapopulations magnifies spatial variability, which creates discrepancies between regional and local trends while increasing risk of local population collapses. Such effects asymmetrically impact locally constrained fishers and predators, which are more exposed to risks of localized collapses. Importantly, we show that dynamically optimizing harvest can minimize local risk without sacrificing yield. Thus, multiple nested scales of management may be necessary to avoid cryptic collapses in metapopulations and the ensuing ecological, social and economic consequences.

Keywords: Sustainable fisheries, Metapopulation, Population Dynamics, Conservation, Natural Resource Management

Introduction

Mismatches in spatial scale create pervasive problems in ecology and natural resource management (Cumming et al. 2006, Cope and Punt 2011). This problem occurs in part because the spatial extent of management or conservation units is often defined by history, jurisdictional, or institutional criteria rather than the scale of social and ecological processes at play (Levin 1992, Chesson 1998, Cumming et al. 2006). Such choices concerning the scale of management can result in spatial mismatches, where feedbacks controlling interactions among groups occur at different scales. In managed ecosystems like forestry and fisheries, mismatches may occur when harvest recommendations are based on trends in large-scale abundance without accounting for localized collapses (Johnson et al. 2012) or spatial variation in population structure and harvest rates (Cope and Punt 2011). Yet these spatially isolated collapses can have far-reaching consequences when the species play an indispensable role in local social-ecological systems, including human communities with limited capacity to forage over wide geographic scales. Empirical identification of appropriate spatial scales of management remains difficult for spatially structured populations, but can be a pre-requisite for diagnosing and reconciling challenges that spatial mismatches impose on the sustainable and equitable use of natural resources.

In metapopulations – plant or animal populations connected through dispersal – it is well established that the dynamics of individual populations can differ substantially from the aggregate metapopulation (Chesson 1998, Mangel and Levin 2005, Melbourne and Chesson 2006). A combination of movement, shared climate drivers, and compensatory processes determine whether dynamics of individual populations reflect the dynamics of the aggregate

47 metapopulation (Kendall et al. 2000). Consideration of metapopulation structure has improved
48 the management of the spotted owl (*Strix occidentalis*) (Lande 1988), salmon (*Onchorhyncus*
49 spp.) (Stephenson 1999, Rieman and Dunham 2000, Schtickzelle and Quinn 2007, Peterson et al.
50 2014), amphibians (Marsh and Trenham 2001), and mosquitoes (Adams and Kapan 2009). To
51 date, efforts to integrate metapopulation dynamics into natural resource management have
52 largely focused on either minimizing the risk of localized extinction (Chadès et al. 2011),
53 characterizing productivity of the metapopulation as a whole (sensu Takashina and Mougi 2015),
54 or valuing benefits of portfolio effects (i.e. stabilizing effects of spatial asynchrony sensu
55 Schindler et al. 2010). Less understood, both in theory and in practice, is if and when harvesting
56 metapopulations can increase spatial variability that yield mismatches in spatial scales of
57 management and population dynamics.
58
59 In this study, we assess how harvest dynamics interact with animal movement and recruitment to
60 shape spatial population variability and risk of collapse at different spatial scales. Our results
61 illustrate the challenge in managing spatially complex populations using three complementary
62 approaches. First, we develop new theory using a stochastic analytical model to examine when
63 and how harvesting in a metapopulation amplifies spatial variability that can create mismatches
64 in spatial scale. Second, we contextualize the problem of spatial variability and mismatches in
65 spatial scale by presenting historical analyses from spatial Pacific herring (*Clupea pallasii*)
66 fisheries in British Columbia, Canada and home-ranges of associated predators and fishers that
67 may be impacted by localized collapses. Finally, we evaluate how and when different harvest
68 management approaches can ameliorate such mismatches using a numerical risk analysis in
69 Pacific herring fisheries.

70

71 ***Pacific herring case study in British Columbia's Central Coast***

72 Pacific herring exemplify the challenges inherent to managing metapopulations that exhibit
73 spatial variation in population trends. In British Columbia (BC), Canada, herring return annually
74 to nearshore coastlines in the late winter/early spring to reproduce. During this annual migration,
75 they are harvested and preyed upon by a range of consumers. Mobile commercial fishing fleets
76 harvest adult herring, largely for their roe, in the days prior to spawning. In contrast, Indigenous
77 fishers are constrained to a local area and largely harvest eggs after spawning events (though
78 some adults as well) as an important food, trade, and cultural resource (Lepofsky and Caldwell
79 2013, McKechnie et al. 2014, Department of Fisheries and Oceans 2015, von der Porten et al.
80 2016, Okamoto et al. 2019). These activities create trade-offs among commercial roe fisheries
81 that remove spawning adults, which truncates adult age structure and reduces abundance, versus
82 those that remove only eggs from shorelines (Shelton et al. 2014). Unfortunately, a core
83 uncertainty for herring management, as for many species, is the extent of movement between
84 areas (Flostrand et al. 2009, Benson et al. 2015, Jones et al. 2016, Levin et al. 2016). Similar
85 uncertainty surrounds spatial variation in spawning biomass (Siple and Francis 2016), which
86 may result in part from the degree of demographic synchrony between areas (e.g. synchrony in
87 recruitment). Pacific herring in British Columbia are currently managed as stocks at regional
88 scales (100s of kilometers) by Canada's federal fisheries agency. Within these stocks, multiple
89 spawning aggregations (substocks) seasonally occupy individual stretches of coastline, many of
90 which are of important traditional and cultural value to Indigenous groups. Thus, Pacific herring
91 fisheries present a valuable system in which to explore how spatial population dynamics, scales

of management, and spatial constraints of fishers and predators interact to influence differential risk exposure to population collapses.

Methods

Methodological Overview

We used three distinct modeling approaches in this study to explore how harvest can affect spatial dynamics in metapopulations. In **Model 1,** we developed a novel analytical approach to modeling stochastic age-structured metapopulations to illustrate how and when harvest can interact with migration and both the magnitude and spatial synchrony of environmental stochasticity. We illustrated these important interactions using this model because of its simplicity and interpretability relative to more complicated nonlinear numerical models. In **Model 2,** we analyzed Pacific herring data from British Columbia using a Bayesian hierarchical model to estimate spatiotemporal variation in spawning biomass and harvest rates. In **Model 3,** to evaluate potential solutions for spatial mismatches and conditions for their success, we developed and applied a spatially explicit stochastic numerical model of metapopulations and their interaction with the fishery. Together, these approaches (Models 1-3) generate theoretical, empirical, and numerical results for understanding the complex, spatially-structured interactions among populations, harvest, and environmental variability. The collective results are then applied to evaluate the consequences for the availability of important natural resources for both human and non-human user groups.

114 ***Theoretical effects of harvest on spatial variability in metapopulations (Model 1)***

115 We used a simple metapopulation model to evaluate how harvest alters spatial variability,
116 conditional on the underlying properties of the metapopulation. For our purposes, spatial
117 variability is the degree to which volatility of the populations are masked by the observed
118 volatility of the metapopulation.

119

120 We considered a simple metapopulation consisting of two populations, linked through the annual
121 fraction migrating between populations (δ). We assumed both populations have the same
122 dynamics (identical density independent adult total mortality rate (Z), maturity at age 2,
123 Gompertz stock-recruit relationship, and symmetric adult annual migration) and trends in
124 recruitment variability are controlled by a spatially correlated lognormal environmental
125 stochasticity.

126

127 Let represent the abundance of age class a at location i at time t *as* $Y_{a,i,t}$. Adult dynamics are
128 shaped by mortality (Z - the sum of mortality from natural causes and harvest) and migration
129 ($0 \leq \delta \leq 0.5$):

130 **Eq. 1:** $$Y_{a,i,t+1} = \begin{cases} e^{-Z}\left[(1-\delta)Y_{a-1,i,t} + \delta Y_{a-1,j,t}\right] & 2 \leq \mathrm{a} \leq \mathrm{n}-1 \\ e^{-Z}\left[(1-\delta)(Y_{a-1,i,t} + Y_{a,i,t}) + \delta(Y_{a-1,j,t} + Y_{a,j,t})\right] & a = \mathrm{n}\ (\text{plus group}) \end{cases}$$

131 Total reproduction is the sum of adults across all adult age classes multiplied by 0.5 to account
132 for an equal sex ratio:

133 **Eq. 2:** $$Y_{\mathrm{a}=0,i,t+1} = 0.5e^{-z}\sum_{a=1}^{n}\left((1-\delta)Y_{a,i,t} + \delta Y_{a,j,t}\right)$$

Both Eq. 1 and 2 are identical for both subpopulations (i.e. the system is symmetrical). We used a stochastic Gompertz model as the compensatory function that determines how zygotes translate into one-year-olds:

Eq. 3: $Y_{\mathrm{a}=1,i,t+1} = \alpha(Y_{\mathrm{a}=0,i,t})^{1-\beta}\mathrm{e}^{\zeta_{i,t}}$

α, β and $\zeta_{i,t}$ represent, respectively, the density independent productivity parameter, the within-location compensatory parameter, and environmental stochasticity that operates on post-dispersing larvae. The vector $\boldsymbol{\xi}_t = [\zeta_{1,t}, \zeta_{2,t}]'$ follows a multivariate normal distribution with mean zero and covariance controlled by the common within-site variance (σ_R^2) and spatial correlation (ρ_R) yielding $\mathrm{cov}[\,\zeta_{1,t}, \zeta_{2,t}] = \begin{bmatrix} \sigma_R^2 & \sigma_R^2\rho_R \\ \sigma_R^2\rho_R & \sigma_R^2 \end{bmatrix}$.

To analyze the stochastic metapopulation model, we converted the model to a first order vector autoregressive model where statistical properties of stochastic forcing in multivariate systems are well described (Lütkepohl 2005). We first vectorized the model by aligning variables from both populations in a single vector:

$\mathbf{Y_t} = [Y_{a=0,L=1,t} \quad \cdots \quad Y_{n,L=1,t} \quad Y_{a=0,L=2,t} \quad \cdots \quad Y_{n,L=2,t}\,]'$

We then cast the model in terms of log-scale deviations from the equilibrium (i.e. $x_{a,i,t} = \ln Y_{a,i,t} - \ln Y_{a,i}^*$ where $Y_{a,i}^*$ is the equilibrium) and linearized about the equilibrium (Nisbet and Gurney 1982, Bjørnstad et al. 2004) to create a first order vector autoregressive model. This approach approximates the deterministic dynamics of the nonlinear model with a Jacobian matrix (**J**) of first order dependencies and an environmental covariance matrix.

155 The matrix of Jacobian coefficients (with plus groups summed at age n) are partial derivatives
156 for each age class within each subpopulation with respect to each other age class in each
157 subpopulation. $\mathbf{J}$ can be represented by the block matrix comprised of matrices describing
158 among and within population age transitions:

159 **Eq. 4**: $\mathbf{J} = \begin{bmatrix} J_1 & J_2 \\ J_2 & J_1 \end{bmatrix}$

160 Where J_1 is within population dynamics and J_2 is among population dynamics defined by:

161 **Eq. 5:** $J_i =$

162
$$\begin{bmatrix} 0 & \frac{D}{1+\sum_{a=1}^{n-1}(e^{-Z})^a} & \frac{D(e^{-Z})}{1+\sum_{a=1}^{n-1}(e^{-Z})^a} & \frac{D(e^{-Z})^2}{1+\sum_{a=1}^{n-1}(e^{-Z})^a} & \cdots & \frac{D(e^{-Z})^{n-2}}{1+\sum_{a=1}^{n-1}(e^{-Z})^a} & \frac{D(e^{-Z})^{n-1}}{1+\sum_{a=1}^{n-1}(e^{-Z})^a} \\ 1-\beta & 0 & 0 & 0 & \cdots & 0 & 0 \\ 0 & D & 0 & 0 & \cdots & 0 & 0 \\ 0 & 0 & D & 0 & \cdots & 0 & 0 \\ \vdots & \vdots & \vdots & \vdots & \ddots & 0 & 0 \\ 0 & 0 & 0 & 0 & \cdots & \frac{D}{(e^{-Z})+1} & \frac{D(e^{-Z})}{(e^{-Z})+1} \end{bmatrix}$$

163 If $J_i = J_1$, $D = (1-\delta)$ and if $J_i = J_2$, $\mathrm{D} = \delta$. Z is the annual total mortality rate and n is the
164 number of age classes. See Appendix S1 for full derivation of the Jacobian and VAR(1)
165 properties. The resulting VAR(1) model is:

166 **Eq. 6**: $\mathbf{x_t} = \mathbf{J}\mathbf{x_{t-1}} + \mathbf{Z}\boldsymbol{\xi_t}$

167 **Eq. 7:** $\mathbf{x_t} = [x_{a=0,L=1,t} \quad \cdots \quad x_{n,1,t} \quad x_{a=0,L=2,t} \quad \cdots \quad x_{n,2,t}\ ]'$

168 $\mathbf{Z}$ is a 2n x 2 binary matrix (2 age classes for each location, two locations) that controls which of
169 the entries in $\mathbf{x}_t$ are subject to stochasticity from $\boldsymbol{\xi_t}$ (i.e. translating the 2x1 vector of location
170 specific stochasticity to a 2n x 1 sparse vector). In this case, only age class 1 (corresponding to
171 the second column of J_1) for each subpopulation is subject to stochasticity.
172

We used the known statistical properties of a VAR(1) model (Lütkepohl 2005) in tandem with the moments of a multivariate lognormal to derive the coefficient of variation for the subpopulations and metapopulation that yields the spatial variation in the metapopulation. Finally, to evaluate how local environmental sensitivity of population growth changes with mortality rate, we used a first-order impulse response analysis (Lütkepohl 2005) to estimate the annual intrinsic growth rate response to a recruitment pulse. The impulse response in our case describes how a recruitment perturbation affects the intrinsic growth rate of each subpopulation. Specifically, it is given by the entry of the 2^{nd} column of the 1^{st} row of the Jacobian matrix in Eq. 5. See Appendix S1 for full derivations and details.

Pacific herring case-study: spatial variability in biomass and catch (Model 2)

To estimate patterns of spatial and temporal variability in herring biomass and harvest rates, we used spawn deposition and harvest data for six major Pacific Herring spawning units that comprise the Central Coast stock in British Columbia, Canada. Briefly, SCUBA surveys are used to estimate herring egg abundance which is converted to total spawning biomass with the assumed conversion of ~100 eggs/g and an equal sex ratio (DFO 2015). For consistency we use the same index as in the DFO stock assessment but in the spatially disaggregated form. Catch (which occurs in the days prior to spawning) is reported by geographic section that are delineated and aggregated geographically. For full description of the time series see DFO (2015) and references therein.

To estimate spatial biomass trends from the survey and harvest time series observations, we used a nonlinear model in a Bayesian hierarchical state-space framework. We assumed survival,

196 reproduction, and competition were location specific. We modeled expected change in biomass
197 in year t+1 using a combined growth and survival model (individual growth and survival from
198 year t) and Gompertz recruitment model (from year t-1, because fish mature at or after age 2 -
199 Table 1, Eq. 8).
200
201 We estimated both process error and observation error in the model. We estimated spatially
202 correlated process error that represents deviations from the expected log-scale pre-harvest
203 biomass within each location. Process error may arise from a diverse combination of factors
204 including immigration or emigration and temporal variation in growth, recruitment, or mortality
205 (Table 1, Eq. 9). We also estimated location-specific observation error (Objective function -
206 Table 1, Eq. 10), and a common survey bias (a "catchability" coefficient quantifying the mean
207 proportion of eggs that are observed in fishery-independent surveys - Table 1, Eq. 10). Thus, we
208 estimated trends conditional on estimated survival, biomass growth, process error covariance,
209 observation error, and survey bias.
210
211 Because we estimated log-scale pre-harvest biomass but observations are of post-harvest
212 biomass and harvested biomass, the model requires a change of variables and thus the posterior
213 requires a Jacobian adjustment of the inverse transform (Gelman et al. 2013, Carpenter et al.
214 2016, Table 1, Eqs 10, 11). See Table 1 for all model equations, parameter definitions, and prior
215 distributions. For details of estimation, posteriors, and model validation, see Appendix S2. We
216 estimated the models using Stan (Stan Development Team 2016b, a) with 3 independent Markov
217 Chains with 1000 iteration chains after 1000 iteration burn-in. We confirmed chain mixing and
218 convergence using Gelman-Rubin statistic ($R<1.01$, Gelman and Rubin 1992) and for mdel

219 adequacy and model fit using posterior predictive checks (see below). Posteriors compared with
220 priors for core parameters are shown in Appendix S2: Fig. S1.
221
222 We used the full model posterior of post-harvest biomass to calculate the following metrics: 1)
223 temporal and spatial variation in biomass (see Appendix S2: Fig. S1), and 2) the exploitation
224 rate. We compared the estimated local harvest rates from the model posterior to the theoretical
225 proportional allocation where fishing mortality is constant in space and an optimized allocation
226 of harvest given the quota (see Appendix S2: Fig. S3 for results, Appendix S3 for methods) and
227 the posterior mean. Here, we defined "optimized allocation" of catch as one that distributes
228 catches in space according to the ideal free distribution (see Appendix S3 for methods). This
229 distribution removes proportionally more biomass from subpopulations with higher biomass and
230 is the spatial allocation of catch that minimizes effort to achieve the overall quota (assuming
231 catch per unit effort is linearly related to biomass).
232
233 ***Solutions for spatial scale mismatches in fished herring metapopulations (Model 3)***
234 We used a stochastic model to simulate how spatial metapopulation dynamics and alternative
235 management scenarios interact to influence risk of collapse at the subpopulation and
236 metapopulation scales under a diverse suite of scenarios. The scenarios we examined include a
237 factorial gradient of 1) annual movement (see Annual adult migration among spawning areas
238 below), 2) environmental recruitment synchrony (the degree of correlation in recruitment in
239 space – see Spatiotemporal Recruitment Dynamics below), 3) a range of harvest rates (see Stock
240 Harvest Quota below), and 4) allocation of harvest in space (see Spatial Harvest Prosecution
241 below). For this analysis, we defined a "collapse" as years with spawning biomass below 20%

of unfished biomass. We used this definition for herring because, 1) it is generally seen as a conservative estimate of biomass below which traditional Indigenous harvest becomes difficult and, 2) it lies below the current closure threshold of 25% unfished biomass. Alternative thresholds defining collapse were also assessed but yielded qualitatively similar results (data not shown).

For all analyses, we simulated 10 populations placed around a hypothetical circular island of arbitrary size, where distances among adjacent populations were equal. Fish spawning at any site in a given year were able to move to any other site in the next year. The probability of migration from one site to another declines as alongshore distance between the locations increases and is controlled by a periodic kernel. Likewise, synchrony in stochastic recruitment among sites decays with distance between locations controlled by a periodic covariance kernel. Stochasticity in dynamics was included in recruitment (spatial and temporal variation), survival (temporal variation only) and movement probabilities (spatial and temporal variance). The order of operations mathematically was 1) recruitment, 2) survival, 3) movement, 4) roe fishery harvest, and 5) spawning. Details of the simulation are outlined below with core equations listed in Table 2 and definitions in Table 3.

Spatiotemporal Recruitment Dynamics

Following the assumptions of the current British Columbia herring assessments (DFO 2015), recruitment of age 2 individuals at location i is a function of eggs produced 2-years prior and local density dependence via a Beverton-Holt model. We allowed recruitment to exhibit both spatial and temporal variability and autocorrelation with a first-order vector autoregressive

model. Spatial correlations in recruitment followed a Gaussian spatial decay with distance (d), and location specific recruitment variability was tuned such that net recruitment variability was approximately constant across scenarios (CV of metapopulation recruitment = 0.8; DFO 2015).

Annual Adult Survival and Migration Among Spawning Areas

All adult survival occurred prior to movement into spawning locations, was constant in space and was randomly drawn from a beta-binomial with mean $\lambda = 0.6$ with coefficient of variation of 0.2 (DFO 2015). Survivors migrated to new spawning locations with a probability that decays with distance from the previous site, controlled by a periodic kernel, tuned to achieve the desired retention rate.

Stock Harvest Quota

We followed the existing harvest control rules of Pacific herring in British Columbia (DFO 2015). The annual biomass harvest quota for the stock ($\widehat{Q}_{t+1}$) was designed to achieve a target harvest rate (H_{Target}) and a minimum spawning escapement (25% of B_0 – the average steady state biomass without fishing). For simplicity and to avoid evaluating stock assessment model performance (which is out of the scope of this study) we assume forecasts are unbiased with no observation noise.

Spatial Harvest Prosecution

We used and compared two spatial fleet allocation scenarios to generate the distribution of spatial commercial roe harvest given the stock quota: 1) the fleet prosecuted the fishery equally in space whereby the absolute harvest was directly proportional to spawning biomass within a

given year (***proportional allocation***) or 2) the fleet was allocated according to the ideal free distribution (IFD) that in theory would optimize catch efficiency if fleets are not spatially constrained (***optimized allocation -*** See Appendix S3 for details in generating the IFD). Here, realized catch was nonlinearly related to spawning biomass, harvesting more from areas with higher biomass and leaving alone areas with lower biomass. See Appendix S3 for methods and results from a third allocation strategy, a random spatial allocation that is more similar to the fleet allocation in the empirical case study. In all cases, fishery selectivity was identical to maturity-at-age reflecting that harvest occurs on mature fish at the spawning grounds.

Simulation details

For each simulation, we 1) evaluated deterministic equilibria without fishing, 2) initiated stochastic forcing of recruitment from the equilibrium for 12 years (allowing the full suite of age classes to be influenced by environmental stochasticity), 3) initiated the fishery in year 13, and 4) recorded performance metrics for years 23-52. We ran 100 replicate simulations for each combination of migration probability and recruitment synchrony. Primary performance metrics summarized for each simulation included a) mean number of years below 20% B_0 at both stock and substock scales to assess risk of collapse, b) mean stock and substock level catch, c) mean stock and substock biomass, d) stock and substock temporal variability (coefficient of variation) in biomass, and e) mean spatial variation in biomass (difference between squared coefficient of variation at the substock versus stock scale).

Results

Theoretical effects of harvest on spatial variability in metapopulations (Model 1)

Our model illustrates that spatial variation among subpopulations increases with higher harvest rates (Fig. 1a) and decreases with synchronizing forces of migration and environmental correlation (difference in surfaces in Fig. 1b). As a result, the metapopulation trend and coefficient of variation are less reflective of trends and variation in its subpopulations as harvest increases (Fig. 1b). Biologically, this higher mortality rate decreases longevity and increases local-scale sensitivity to spatially explicit recruitment pulses. The amplification of fluctuations occurs at a higher rate at local scales than on aggregate. This response decreases spatial coupling and predictability. Reduced longevity of adults (via higher mortality) reduces the abundance of adults in each subpopulation that buffers against local stochasticity through survival and migration.

Mathematically, this result emerges for several related reasons. Increases in mortality (constant across space in this case) reduce local subpopulation inertia (predictability, measured as 1st order temporal autocorrelation, thick black line in Fig. 1c). This reduction in inertia increases subpopulation sensitivity to temporal variation in local subpopulation recruitment (red line in Fig. 1c). This sensitivity is illustrated by the primary impulse response at a single lag which in this case always increases with total mortality (Z) derived from Eq. 5:

Eq. 22: $$(1-\delta)/(1+\sum_{a=1}^{n-1}(e^{-Z})^{a})$$

330 Such increases in local environmental sensitivity reduce spatial coupling (measured as the spatial
331 autocorrelation, dotted black line in Fig. 1c) and thereby increase spatial variability in
332 abundance.
333
334 Importantly these patterns of spatial variability can persist even in the presence of modest
335 migration rates (Fig. 1b). While spatial variability decreases with synchronizing forces of
336 migration (δ) and environmental correlations (ρ_R) (Fig. 1b, see Appendix S1 for solutions),
337 spatial variability only diminishes as migration and environmental correlations are substantially
338 high (i.e. as migration probabilities approach 0.5 to produce 100% mixing). This phenomenon
339 is illustrated by the discrepancies between temporal variability of the metapopulation and
340 component subpopulations that produce spatial variation (Fig. 1b).
341
342 Next we illustrate challenges imposed by spatial variation in exploited metapopulations using an
343 empirical case study of Pacific herring and present solutions using a numerical management
344 strategy evaluation.
345
346 ***Pacific herring case-study: spatial variability in biomass and catch (Model 2)***
347 Pacific herring subpopulations on the Central Coast of BC exhibit substantial spatial variability
348 in subpopulation trends (Fig. 2a, b, c). The estimated biomass of individual ("local")
349 subpopulations has varied by more than an order of magnitude over the past three decades, and
350 similar differences in biomass are evident among subpopulations in the same year. As a
351 consequence, aggregate ("regional") stock biomass at any one point in time is bolstered by a few
352 subpopulations, while others linger at low levels (Fig. 2b, Appendix S2: Fig. S2). Synchrony in

353 biomass among subpopulations is low (0.29), with much higher variability at the subpopulations
354 scale (average CV = 0.88) than in aggregate (CV = 0.54). This discrepancy results from high
355 spatial variability in subpopulations trends (Fig. 1c - also known as β variability; (Wang and
356 Loreau 2014). In fact as much as an estimated 91% of an individual subpopulation's biomass is
357 harvested annually, though the aggregate exploitation rate fluctuates around the target of 20%
358 (Fig. 2d, e, Appendix S2: Fig. S3). Counterproductively, this can result in occurrences where
359 subpopulations experiencing periods of lower-than-average biomass are heavily exploited
360 preceding collapse (e.g. Fig. 2d, in 2006). Harvest rates generally differ in magnitude among
361 subpopulations in any given year (Appendix S2: Fig. S3) and higher harvest rarely focus on the
362 subpopulations with highest biomass (Appendix S2: Fig. S3). This is illustrated directly by
363 spatial harvest distributions that deviate substantially from baselines of spatial harvest evenness
364 used here and in the simulation model (proportional vs optimized allocation - Appendix S2: Fig.
365 S3). Next we explore the potential consequences of different spatial harvest distributions via a
366 closed-loop simulation model.
367
368
369 ***Solutions for spatial scale mismatches in fished herring metapopulations (Model 3)***
370 We used numerical simulation of a metapopulation to determine whether and under what
371 conditions exploitation rates that appear sustainable in aggregate can risk collapse of local
372 subpopulations, and by extension, adversely affect predators and the fishers who target them at
373 this scale. The divergence in risk among scales, an effect of the mismatch in spatial scale, is
374 controlled by the magnitude of harvest rates, allocation of harvest in space, annual migration,
375 and spatial recruitment synchrony. Our simulations show that risk of collapse can be 10 times

376 greater at local subpopulation scales than at aggregate metapopulation scales (Fig. 3) for the 20%
377 harvest rule. While it may seem intuitive that relatively modest adult migration would minimize
378 differences in risk to subpopulations and the metapopulation, our results do not support this
379 supposition. Even relatively high migration rates can impose substantial discrepancies in the risk
380 of collapse between subpopulation and metapopulation scales (Fig. 3). This principle holds so
381 long as spatial synchrony in recruitment is not exceedingly high (Fig. 3 upper portions of
382 heatmaps). For most scenarios, high spatial variability (i.e. from low annual migration among
383 subpopulations or low spatial recruitment synchrony) leads to low apparent risk at the aggregate
384 metapopulation scale, despite high risk of collapse for local subpopulations (Fig. 3; risk increases
385 towards the lower left quadrants).
386
387 We find that risk to local subpopulations greatly exceeds risk to the aggregate metapopulation
388 with both a simulated 10% and 20% target harvest rate. Under the 20% target harvest, risk of
389 collapse at the local scale exceeds 10%, even with annual migration among subpopulations
390 approaching 50% (Fig. 3 h). When harvest is optimized in space or target harvest rates are
391 reduced to 10%, risks of collapse at local scales are substantially reduced (Fig. 3 d,f,j versus Fig.
392 3 h) and limited to scenarios where migration is ~10-15% and spatial synchrony in recruitment is
393 low. Local scale risks of collapse are even worse under a random (or opportunistic) spatial
394 allocation, but also ameliorated by reductions in harvest (Appendix S3: Fig. S2). Importantly, a
395 10% target harvest with optimized spatial allocation never exceeded 10% risk of collapse in our
396 simulations.
397

398 The discrepancy in risk of collapse at local subpopulation versus aggregate metapopulation
399 scales is shaped by both overall harvest rates and spatial variance in subpopulation trend (Fig.
400 S5). Risk at the subpopulation scale matches that of metapopulation scales when subpopulations
401 exhibit little spatial variance (i.e. when there is high recruitment synchrony or high migration,
402 top vs bottom panels in Fig. 3 c-j, SI Fig. S6). In contrast, risk diverges with increases in spatial
403 variance (Fig. S5). Spatial variance is shaped not only by spatial recruitment synchrony and
404 migration, but also harvest rates and allocation in space. Fig. 4b-c illustrates how different
405 harvest allocations impact spatial variation in trends (Fig. 4 d, e). Higher harvest rates increase
406 risk at subpopulation scales in part because of higher depletion at the metapopulation scale (Fig.
407 3 d,f,h,i) and also because harvest can increase spatial variance (Fig. 4d, also explored more
408 generally in Fig. 1) when efforts are allocated proportionally. This result demonstrates how low
409 demographic synchrony creates a portfolio effect at the metapopulation scale but simultaneously
410 masks risks of collapse at the subpopulation scale which can be exacerbated with higher harvest
411 rates.
412
413 However, dynamically optimizing harvest rates in space to match local scale variability lowers
414 the risk of subpopulation and aggregate metapopulation collapse (Fig. 3 d vs f and Fig. 3 h vs i)
415 with no cost to aggregate catch (Appendix S3: Fig. S3). These results emerge from simulating a
416 form of spatially optimized fishing effort that leaves underperforming locations unexploited and
417 heavily targets overperforming local subpopulations, in accordance with predictions of ideal free
418 distribution theory. Optimal spatial allocation of harvest rates reduces the effects of harvest
419 intensity on spatial variability (Fig. 4d) which is strongly related to the bias in estimating risk
420 among scales (Appendix S3: Fig. S1) and also reduces length of individual collapses (Appendix

S3: Fig. S3). Thus, approaches that optimize spatial harvest to account for subpopulation dynamics can minimize the spatially destabilizing effect of harvest as well as disparity in exposure to risk of collapse among spatial scales. The benefits of spatially optimized harvest in terms of risk to subpopulations diminishes as migration and spatial synchrony in recruitment productivity decline to low levels (i.e. approach the lower left quadrant of panels in Fig. 3 d,f,h,j, where subpopulations are nearly autonomous with low connectivity).

Discussion

Harvest strategies that appear appropriately prescribed at large spatial scales can, at local scales, lead to declines or even effective extirpation of local subpopulations. We call these small-scale declines "cryptic collapses". Specifically, regional harvest strategies can create a "gilded trap" (Steneck et al. 2011) where, in this case, management focuses on the aspects of metapopulations that can benefit conservation and economics at the aggregate scale, but neglect social-ecological inequity in the exposure to risk at local scales. Our results show that spatial mismatch among scales is not merely an esoteric concern. Indeed, they occur in current management situations, and are supported by ecological theory we develop here. Our multiscale risk analysis highlights the impacts of scale mismatch on consumers and the potential value of optimized spatial management for sustainability and equity. Previous studies have also investigated spatial mismatches in fisheries contexts to understand consequences stemming from spatial mismatches among biological processes and available data, as well as the spatial implementation of fisheries for yield and measure of population status assessments (Cope and Punt 2011, McGilliard et al. 2011, Spies et al. 2015, McGilliard et al. 2017). Our work expands on previous investigations by considering how spatial dynamics of fish and fisheries affect resource sustainability at multiple

444 spatial scales that are relevant to different species and fishing communities. Our models address
445 this gap by building on existing research with increased biological realism to allow for 1) adult
446 migration rates among subpopulations rather than only dispersal associated with recruitment (e.g.
447 Cope and Punt 2011, McGilliard et al. 2011, Spies et al. 2015, McGilliard et al. 2017) ; 2) a
448 range of complex spatio-temporal correlations in the stochastic populations dynamics (but see
449 McGilliard et al. 2011 for an implementation of spatio-temporal variation in adult mortality); and
450 3) a novel suite of fisheries spatial harvest strategies.
451
452 *Insights into the benefits of population portfolios to manage risk for different groups*
453
454 Our work adds critical resolution and understanding to the literature on portfolio effects that is
455 focused on the benefits of spatial variability. Recent work viewing multiple populations as a
456 "portfolio" of assets has shown benefits of maintaining a diversity of subpopulations with high
457 asynchrony. These benefits include reducing local extinctions through so called 'rescue effects'
458 (Hill et al. 2002, Secor et al. 2009, Fox et al. 2017), providing increased stability in the form of
459 food security for people or animals (Nesbitt and Moore 2016) and minimizing economic risks
460 over large scales by minimizing variance in harvestable abundance (Schindler et al. 2010). Yet
461 these portfolio analyses typically focus on the attributes of the aggregate metapopulation,
462 whereas the risk of localized subpopulation collapse (e.g. depletion below a threshold of
463 ecological functionality or socioeconomic value) affects the interests of locally constrained
464 fishers and spatially constrained organisms with small home ranges. Using theory and data we
465 show that the same spatial variation that leads to resilience at the metapopulation scale, when left

466 unaccounted for in management strategies, can also produce unforeseen negative consequences
467 in the form of magnified spatial variation and local risk of collapse (see also Spies et al. 2015).
468
469 In the case of Pacific herring in the Central Coast of British Columbia, local reductions in some
470 subpopulations occurred well before the entire stock showed substantial declines in the mid-
471 2000s. These collapses had greater impact on spatially constrained groups; namely Indigenous
472 communities for whom herring is a source of cultural and economic vitality (Brown and Brown
473 2009, Gavreau et al. 2017). In contrast, mobile fishing fleets and transient predators should be
474 less vulnerable to local depletion events in the short term. Such context dependent effects of
475 ignoring spatial variation are exemplified through considering the dramatic differences in the
476 spatial scale at which predators and fishers operate. Indigenous fishers are spatially constrained
477 by boat size, fuel costs, and political/cultural boundaries (Fig 2a, Table 4, Harris 2000, von der
478 Porten et al. 2016). In contrast, the commercial fleet of seine and gillnet fishers are highly mobile
479 and can pursue fish throughout the region. Similarly, non-human predators of herring and
480 herring roe have a diversity of home-ranges and therefore interact with herring at multiple scales
481 (Table 4). Many predators rely on herring when they move inshore around spawning season.
482 Many crustaceans (Hines 1982, Stone and O'Clair 2001), echinoderms (Mattison et al. 1976,
483 Cieciel et al. 2009), rockfishes and lingcod (Jorgensen et al. 2006, Mitamura et al. 2009,
484 Tolimieri et al. 2009, Beaudreau and Essington 2011, Green and Starr 2011, Freiwald 2012),
485 harbor seals (Peterson et al. 2012, Ward et al. 2012), some seabirds (Peery et al. 2009, Barbaree
486 et al. 2015, Lorenz et al. 2017), and some flatfishes (Moser et al. 2013), exhibit restricted
487 patterns of movement and are likely to exploit one to several major subpopulations, but generally
488 not the entire spatial distribution of the metapopulation (stock). In contrast, humpback whales

(Dalla Rosa et al. 2008, Kennedy et al. 2014), orcas (Hauser et al. 2007, Fearnbach et al. 2014), some seabirds (Pearce et al. 2005), sea lions (Merrick and Loughlin 1997, Fearnbach et al. 2014, Kuhn and Costa 2014), fur seals (Kuhn et al. 2014), halibut (Loher 2008, Seitz et al. 2011, Nielsen et al. 2014), and gadiforms (Wespestad et al. 1983, Hanselman et al. 2014, Rand et al. 2014) can, given ranges reported, access the geographic area covered by the stock (Table 4, see DataS1:Appendix S4). Thus, herring provide food resources to groups with varying movement constraints. As a result, herring collapses that range from small-scale subpopulations to metapopulation-wide phenomena may have differential impacts on the diverse predators that depend on this resource. These spatial scale dependencies affect which fishing communities or species bear the brunt of management risks and who reaps the benefits from the portfolio payoff of regional metapopulation stability. These outcomes highlight that ignoring space can exclude critical social, ecological, and economic responses central to the triple bottom line (Elkington 1994, Okamoto et al. 2019).

Pacific herring fisheries on Canada's west coast provide an empirical case where the scale of regional stock assessments masked episodic local overexploitation and subpopulation collapses. Here, high local harvest rates appear to be commonplace even when local subpopulations are depleted presumably because of at least two key factors. First, schooling fish are easy to catch even at low abundances (Mackinson et al. 1997) and thus the quota is likely to be achieved even if the abundance of spawning fish in a particular location is small. Second, managers are challenged with fulfilling quotas with imperfect spatial information about spawning abundances. While high local harvest rates may have contributed to subsequent local collapses observed in this case study, quantifying other confounding demographics (i.e. spatial variation in stochastic

adult mortality) are necessary to explicitly test this hypothesis. While recent local collapses may have occurred in the absence of fishing, fishing is very likely imposing higher subpopulation sensitivity to any environmental or biotic influence on recruitment or survival by reducing adult longevity thereby eroding an important buffer against recruitment volatility (Essington et al. 2015) that we show can contribute to spatial variation. Importantly, spatial variation may not only affect the localized groups. In the long term, assumptions of spatial homogeneity can generate biased estimates of total productivity (Takashina and Mougi 2015) that may lead to overly optimistic harvest strategies. Thus, high local harvest rates may produce sequential depletion over time that eventually erodes the principal of the stock with potential to generate collapse of the portfolio as a whole (Spies et al. 2015).

Linking harvest dynamics to spatial variation in population dynamics

Importantly, spatial variation in population dynamics is not independent of harvest dynamics. Rather, we demonstrate numerically and analytically that spatial variation is likely to increase with harvest. This can occur in part because harvesting reduces spatial coupling. Higher mortality is known to reduce the abundance of older age classes (Barnett et al. 2017) and increase sensitivity to fluctuations in recruitment (Beddington and May 1977, Bjørnstad et al. 2004, Hsieh et al. 2006, Shelton and Mangel 2011, Okamoto et al. 2016). In spatially structured systems, such reduced longevity diminishes the synchronizing effect of migration and elevates sensitivity of subpopulations to localized environmental effects. However, if the distribution of harvest in space can be optimized to more adequately accommodate the spatial distribution of fish, we show how the overall portfolio can benefit at multiple scales. Here, demographic

535 asynchrony (in this case asynchrony in recruitment productivity) can be maintained while
536 minimizing subpopulation risk. Translated into practice, our simulation and analytical results
537 highlight two non-mutually exclusive solutions that provide more equitable spreading of risk
538 among scales. First, reductions in overall harvest rates can ameliorate biases in risk among
539 scales. This occurs by reducing baseline levels of risk and reducing effects of harvest on spatial
540 variability. Second, spatially optimizeing harvest allocations can minimize spatial variance and
541 ease pressure on at-risk subpopulations, thereby reducing risk of local scale depletion without
542 sacrificing catch. The first solution creates a trade-off between commercial yield and local risk;
543 the second solution between the costs of management and fleet transportation, and local risk of
544 subpopulation collapse. Specifically, achieving something similar to the latter (second solution)
545 in a realistic setting is likely to require either some combination of greater investment in spatial
546 monitoring, spatial stock assessments (Punt et al. 2018), and in season-management. Thus,
547 moving in the direction of spatial optimization is likely to require substantial investment in costs
548 and personnel for research, stock assessment, and management.
549
550 Addressing spatial inequity in risk exposure requires confronting these economic and logistical
551 trade-offs. For species such as Pacific herring that have volatile spatiotemporal dynamics and
552 complex migratory phenology (Benson et al. 2015), polycentric governance structures where
553 governing authorities are nested at different spatial scales may help balance these trade-offs by
554 addressing the problems of fit between ecosystems, social systems, and management agencies
555 (Young 2002, Berkes 2006, Borgström et al. 2006, Folke et al. 2007, Biggs et al. 2012, von der
556 Porten et al. 2016). Such systems can capitalize on scale-specific ecological knowledge
557 (including local, traditional, and scientific knowledge), scientific capacity and socioeconomic

558 experience to 1) guide decision analyses, 2) co-coordinate data collection and harvest allocation
559 in space, and 3) test policies (e.g. in the Maine Lobster fishery (Acheson 2003)). Polycentric
560 management schemes, however, are not a silver bullet. For systems like Pacific herring where
561 placed-based Indigenous fishing communities often object to purely centralized scales of
562 management for social, ecological, and economic reasons (Brown and Brown 2009, Thornton
563 and Kitka 2015, von der Porten et al. 2016, Gavreau et al. 2017, von der Porten et al. 2019),
564 opportunities to integrate knowledge and objectives into management strategies (and their
565 evaluation) at smaller spatial scales is well placed in managing these fisheries, and may be
566 critical to their perpetuity (Okamoto et al. 2019, Salomon et al. 2019).
567
568 The models used to generate inference in this study are simple in comparison to the nature of
569 complex stochastic systems in space. The analytical model (Model 1) makes numerous
570 simplifications (linearization, biological simplicity) in order to generate analytical and
571 generalizeable solutions but may ignore more nuanced nonlinearities. The numerical model
572 (Model 3) on the other hand is more detailed but outcomes are context dependent. Moreover,
573 both models ignore many biological and management scenarios that are likely to further
574 complicate spatial patterns (e.g. behaviorally or geographically complex migration (MacCall et
575 al. 2018, Rogers et al. 2018), spatial and age specific mortality (McGilliard et al. 2011), spatially
576 complex density dependence (McGilliard et al. 2017), Allee effects, cost, and data limitations for
577 spatial management). We also ignore many alternative spatial allocation strategies that may be
578 explicitly designed to maximize long-term yields or minimize spatiotemporal variability in part
579 because these approaches would require a spatial assessment model, which is out of the scope of
580 this study. However, the principles from our simulation and analytical models should generalize

581 regardless of the degree of complexity in the system: a precautionary approach cognizant of
582 resource users across multiple spatial scales may necessitate the incorporation of some degree of
583 locally based management to minimize spatial discrepancies in risk exposure. Our results
584 highlight the need to consider diverse scenarios and incorporate fundamental biological attributes
585 that may impact resource dynamics and people at different scales. Overall, our models suggest a
586 mixture of management scales may be key to selecting and coordinating harvest levels in space
587 to navigate towards sustainable and equitable outcomes (Cope and Punt 2011, Biggs et al. 2012).
588
589 *Conclusion*
590
591 Our analyses illustrate the importance of considering spatial dynamics for determining how to
592 most effectively balance equity in management and conservation strategies aimed at achieving
593 social, economic, and ecological outcomes (Halpern et al. 2013, Law et al. 2017). These issues
594 are often ignored by centralized management and conservation initiatives focused on larger
595 spatial scales. For over half a century, fisheries scientists have debated how best to exploit and
596 conserve "mixed stocks" that have separate dynamics but are inseparable in space, with the aim
597 of balancing conservation of weak stocks and maximizing total yields (Ricker 1958). Our work
598 inverts this focus to metapopulations where subpopulations have inseparable dynamics but are
599 separated in space. We show how, in these settings, exploitation can magnify local scale
600 fluctuations and spatial variability. As a result, aggregate metrics poorly represent local scale
601 dynamics and the risk of collapse at the local scale increases at a greater rate than the aggregate
602 large scale. This phenomenon creates cryptic collapses with ensuing discrepancies in risk
603 exposure. Fortunately, the magnitude of these discrepancies can potentially be controlled by

lowering harvest rates or seeking harvest dynamics that are spatially optimized. Overall, these conclusions are relevant not only to Pacific herring fisheries, but also to the great number of exploited natural resources that exhibit spatial structure and are valuable to species and people that operate on multiple scales.

Acknowledgements:

DKO was supported by a Strategic Partnership Grant from the National Sciences and Engineering Research Council (NSERC) of Canada to AKS and MHL and a first-year assistant professor (FYAP) award to DKO from the FSU Council on Research and Creativity. We thank the Gordon and Betty Moore Foundation for their support of AS, JSF, PSL, the Ocean Tipping Points project and the David and Lucille Packard Foundation for their support of PSL, the Tula Foundation for their support of MHL, and the Ocean Modeling Forum. We thank J. Cleary, S. Harper, M. Reid, K. Gladstone, B. Gladstone, K. Brown, and D. Neasloss for discussions that initiated and refined the research, A. Frid and A. Rassweiler for input on the manuscript, and S. Cox, L. Dee, L. Hauser, B. Hunt, S. Miller, I. McKechnie, S. Pau, T. Pitcher, E. Petrou, T. Francis, A. Punt and W. Smith for discussions that improved the research. We also thank the Heiltsuk and Haida First Nations for their partnership in the NSERC Strategic Partnership Grant and the Department of Fisheries and Oceans for providing herring spatial data.

627 **References**

628 Acheson, J. M. 2003. Capturing the commons: Devising institutions to manage the maine lobtser
629 industry. University Press New England, Lebanon, NH.

630 Adams, B., and D. D. Kapan. 2009. Man bites mosquito: understanding the contribution of
631 human movement to vector-borne disease dynamics. PloS one 4:e6763.

632 Barbaree, B. A., S. Nelson, and B. D. Dugger. 2015. Marine space use by marbled murrelets
633 Brachyramphus marmoratus at a mainland fjord system in southeast Alaska. Marine
634 Ornithology 116:173-184.

635 Barnett, L. A., T. A. Branch, R. A. Ranasinghe, and T. E. Essington. 2017. Old-Growth Fishes
636 Become Scarce under Fishing. Current Biology 27:2843-2848. e2842.

637 Beaudreau, A., and T. Essington. 2011. Use of pelagic prey subsidies by demersal predators in
638 rocky reefs: insight from movement patterns of lingcod. Marine biology 158:471-483.

639 Beddington, J. R., and R. M. May. 1977. Harvesting natural populations in a randomly
640 fluctuating environment. Science 197:463-465.

641 Benson, A. J., S. P. Cox, and J. S. Cleary. 2015. Evaluating the conservation risks of aggregate
642 harvest management in a spatially-structured herring fishery. Fisheries Research 167:101-
643 113.

644 Berkes, F. 2006. From community-based resource management to complex systems: The scale
645 issue and marine commons. Ecology and Society 11.

646 Biggs, R., M. Schluter, D. Biggs, E. L. Bohensky, S. BurnSilver, G. Cundill, V. Dakos, T. M.
647 Daw, L. S. Evans, K. Kotschy, A. M. Leitch, C. Meek, A. Quinlan, C. Raudsepp-Hearne,
648 M. D. Robards, M. L. Schoon, L. Schultz, and P. C. West. 2012. Toward Principles for

649 Enhancing the Resilience of Ecosystem Services. Annual Review of Environment and
650 Resources 37:421-448.
651 Bjørnstad, O. N., R. M. Nisbet, and J. Fromentin. 2004. Trends and cohort resonant effects in
652 age-structured populations. Journal of animal ecology 73:1157-1167.
653 Borgström, S., T. Elmqvist, P. Angelstam, and C. Alfsen-Norodom. 2006. Scale mismatches in
654 management of urban landscapes. Ecology and Society 11.
655 Brown, F., and Y. K. Brown. 2009. Staying the course, staying alive - coastal First Nations
656 fundamental truths: biodiversity, stewardship and sustainability. Biodiversity BC.,
657 Victora, BC.
658 Carpenter, B., A. Gelman, M. Hoffman, D. Lee, B. Goodrich, M. Betancourt, M. A. Brubaker, J.
659 Guo, P. Li, and A. Riddell. 2016. Stan: A probabilistic programming language. Journal of
660 Statistical Software 20.
661 Chadès, I., T. Martin, S. Nicol, M. Burgman, H. Possingham, and Y. Buckley. 2011. General
662 rules for managing and surveying networks of pests, diseases, and endangered species.
663 Proceedings of the National Academy of Sciences 108:8323-8328.
664 Chesson, P. 1998. Spatial scales in the study of reef fishes: a theoretical perspective. Australian
665 Journal of Ecology 23:209-215.
666 Cieciel, K., B. J. Pyper, and G. L. Eckert. 2009. Tag retention and effects of tagging on
667 movement of the giant red sea cucumber Parastichopus californicus. North American
668 Journal of Fisheries Management 29:288-294.
669 Cope, J. M., and A. E. Punt. 2011. Reconciling stock assessment and management scales under
670 conditions of spatially varying catch histories. Fisheries Research 107:22-38.

671 Cumming, G., D. H. Cumming, and C. Redman. 2006. Scale mismatches in social-ecological
672 systems: causes, consequences, and solutions. Ecology and Society 11.
673 Dalla Rosa, L., E. Secchi, Y. Maia, A. Zerbini, and M. Heide-Jørgensen. 2008. Movements of
674 satellite-monitored humpback whales on their feeding ground along the Antarctic
675 Peninsula. Polar Biology 31:771-781.
676 Department of Fisheries and Oceans. 2015. Stock Assessment and Management Advice for BC
677 Pacific Herring: 2015 Status and 2016 Forecast. . Can. Sci. Adv. Sec. Res. Doc 2015/038.
678 Elkington, J. 1994. Towards the sustainable corporation: Win-win-win business strategies for
679 sustainable development. California management review 36:90-100.
680 Essington, T. E., P. E. Moriarty, H. E. Froehlich, E. E. Hodgson, L. E. Koehn, K. L. Oken, M. C.
681 Siple, and C. C. Stawitz. 2015. Fishing amplifies forage fish population collapses.
682 Proceedings of the National Academy of Sciences 112:6648-6652.
683 Fearnbach, H., J. W. Durban, D. K. Ellifrit, J. M. Waite, C. O. Matkin, C. R. Lunsford, M. J.
684 Peterson, J. Barlow, and P. R. Wade. 2014. Spatial and social connectivity of fish-eating
685 "Resident" killer whales (*Orcinus orca*) in the northern North Pacific. Marine biology
686 161:459-472.
687 Flostrand, L. A., J. F. Schweigert, K. S. Daniel, and J. S. Cleary. 2009. Measuring and modelling
688 Pacific herring spawning-site fidelity and dispersal using tag-recovery dispersal curves.
689 ICES Journal of Marine Science 66:1754-1761.
690 Folke, C., L. Pritchard, F. Berkes, J. Colding, and U. Svedin. 2007. The problem of fit between
691 ecosystems and institutions: Ten years later. Ecology and Society 12.
692 Fox, J. W., D. Vasseur, M. Cotroneo, L. Guan, and F. Simon. 2017. Population extinctions can
693 increase metapopulation persistence. Nature ecology & evolution 1:1271.

694 Freiwald, J. 2012. Movement of adult temperate reef fishes off the west coast of North America.
695 canadian Journal of Fisheries and aquatic Sciences 69:1362-1374.
696 Gavreau, A., D. Lepofsky, M. Rutherford, and M. Reid. 2017. “Everything revolves around the
697 herring”: The Heiltsuk-herring relationship through time. Ecology and Society 22.
698 Gelman, A., and D. B. Rubin. 1992. Inference from iterative simulation using multiple
699 sequences. Statistical science 7:457-472.
700 Gelman, A., H. S. Stern, J. B. Carlin, D. B. Dunson, A. Vehtari, and D. B. Rubin. 2013. Bayesian
701 data analysis. Chapman and Hall/CRC.
702 Green, K. M., and R. M. Starr. 2011. Movements of small adult black rockfish: implications for
703 the design of MPAs. Marine Ecology Progress Series 436:219-230.
704 Halpern, B. S., C. J. Klein, C. J. Brown, M. Beger, H. S. Grantham, S. Mangubhai, M.
705 Ruckelshaus, V. J. Tulloch, M. Watts, C. White, and H. P. Possingham. 2013. Achieving
706 the triple bottom line in the face of inherent trade-offs among social equity, economic
707 return, and conservation. Proceedings of the National Academy of Sciences 110:6229-
708 6234.
709 Hanselman, D. H., J. Heifetz, K. B. Echave, and S. C. Dressel. 2014. Move it or lose it:
710 movement and mortality of sablefish tagged in Alaska. Canadian Journal of Fisheries and
711 Aquatic Sciences 72:238-251.
712 Harris, D. C. 2000. Territoriality, aboriginal rights, and the Heiltsuk spawn-on-kelp fishery. U.
713 Brit. Colum. L. Rev. 34:195.
714 Hauser, D. D., M. G. Logsdon, E. E. Holmes, G. R. VanBlaricom, and R. W. Osborne. 2007.
715 Summer distribution patterns of southern resident killer whales *Orcinus orca*: core areas
716 and spatial segregation of social groups. Marine Ecology Progress Series 351:301-310.

717 Hill, M. F., A. Hastings, and L. W. Botsford. 2002. The effects of small dispersal rates on
718 extinction times in structured metapopulation models. The American Naturalist 160:389-
719 402.
720 Hines, A. H. 1982. Coexistence in a kelp forest: size, population dynamics, and resource
721 partitioning in a guild of spider crabs (Brachyura, Majidae). Ecological Monographs
722 52:179-198.
723 Hsieh, C., C. S. Reiss, J. R. Hunter, J. R. Beddington, R. M. May, and G. Sugihara. 2006.
724 Fishing elevates variability in the abundance of exploited species. Nature 443:859-862.
725 Johnson, T., J. Wilson, C. Cleaver, and R. Vadas. 2012. Social-ecological scale mismatches and
726 the collapse of the sea urchin fishery in Maine, USA. Ecology and Society 17.
727 Jones, R., C. Rigg, and E. Pinkerton. 2016. Strategies for assertion of conservation and local
728 management rights: A Haida Gwaii herring story. Marine Policy.
729 Jorgensen, S. J., D. M. Kaplan, A. P. Klimley, S. G. Morgan, M. R. O'Farrell, and L. W.
730 Botsford. 2006. Limited movement in blue rockfish *Sebastes mystinus*: internal structure
731 of home range. Marine Ecology Progress Series 327:157-170.
732 Kendall, B. E., O. N. Bjørnstad, J. Bascompte, T. H. Keitt, and W. F. Fagan. 2000. Dispersal,
733 environmental correlation, and spatial synchrony in population dynamics. The American
734 Naturalist 155:628-636.
735 Kennedy, A. S., A. N. Zerbini, B. K. Rone, and P. J. Clapham. 2014. Individual variation in
736 movements of satellite-tracked humpback whales *Megaptera novaeangliae* in the eastern
737 Aleutian Islands and Bering Sea. Endangered Species Research 23:187-195.

738 Kuhn, C., R. Ream, J. Sterling, J. Thomason, and R. Towell. 2014. Spatial segregation and the
739 influence of habitat on the foraging behavior of northern fur seals (Callorhinus ursinus).
740 Canadian journal of zoology 92:861-873.
741 Kuhn, C. E., and D. P. Costa. 2014. Interannual variation in the at-sea behavior of California sea
742 lions (*Zalophus californianus*). Marine Mammal Science 30:1297-1319.
743 Lande, R. 1988. Demographic models of the northern spotted owl (Strix occidentalis caurina).
744 Oecologia 75:601-607.
745 Law, E. A., N. J. Bennett, C. D. Ives, R. Friedman, K. J. Davis, C. Archibald, and K. A. Wilson.
746 2017. Equity trade-offs in conservation decision making. Conservation Biology.
747 Lepofsky, D., and M. Caldwell. 2013. Indigenous marine resource management on the
748 Northwest Coast of North America. Ecological Processes 2:1-12.
749 Levin, P. S., T. B. Francis, and N. G. Taylor. 2016. Thirty-two essential questions for
750 understanding the social–ecological system of forage fish: the case of Pacific Herring.
751 Ecosystem Health and Sustainability 2.
752 Levin, S. A. 1992. The problem of pattern and scale in ecology: the Robert H. MacArthur award
753 lecture. Ecology 73:1943-1967.
754 Lewandowski, D., D. Kurowicka, and H. Joe. 2009. Generating random correlation matrices
755 based on vines and extended onion method. Journal of multivariate analysis 100:1989-
756 2001.
757 Loher, T. 2008. Homing and summer feeding site fidelity of Pacific halibut (*Hippoglossus*
758 *stenolepis*) in the Gulf of Alaska, established using satellite-transmitting archival tags.
759 Fisheries Research 92:63-69.

760 Lorenz, T. J., M. G. Raphael, T. D. Bloxton, and P. G. Cunningham. 2017. Low breeding
761 propensity and wide-ranging movements by marbled murrelets in Washington. Journal of
762 Wildlife Management 81:306-321.
763 Lütkepohl, H. 2005. New introduction to multiple time series analysis. Springer, Berlin.
764 MacCall, A., T. Francis, D. Armitage, J. Cleary, S. Dressel, R. Jones, H. Kitka, L. Lee, J.
765 McIsaac, P. Levin, D. Okamoto, M. Poe, A. Punt, S. Reifenstuhl, A. Shelton, M. Miple,
766 J. Silver, J. Schmidt, T. Thornton, R. Voss, and J. Woodruff. 2018. A heuristic model of
767 learned migration behavior exhibits distinctive spatial and reproductive dynamics. ICES
768 Journal of Marine Science. 76:598-608.
769 Mackinson, S., U. R. Sumaila, and T. J. Pitcher. 1997. Bioeconomics and catchability: fish and
770 fishers behaviour during stock collapse. Fisheries Research 31:11-17.
771 Mangel, M., and P. S. Levin. 2005. Regime, phase and paradigm shifts: making community
772 ecology the basic science for fisheries. Philosophical Transactions of the Royal Society
773 B: Biological Sciences 360:95-105.
774 Marsh, D. M., and P. C. Trenham. 2001. Metapopulation dynamics and amphibian conservation.
775 Conservation biology 15:40-49.
776 Martell, S., J. Schweigert, V. Haist, and J. Cleary. 2012. Moving towards the sustainable
777 fisheries framework for Pacific herring: data, models, and alternative assumptions; Stock
778 Assessment and Management Advice for the British Columbia Pacific Herring Stocks:
779 2011 Assessment and 2012 Forecasts. Can. Sci. Adv. Sec. Res. Doc 136:163.
780 Mattison, J., J. Trent, A. Shanks, T. Akin, and J. Pearse. 1976. Movement and feeding activity of
781 red sea urchins (*Strongylocentrotus franciscanus*) adjacent to a kelp forest. Marine
782 Biology 39:25-30.

783 McGilliard, C. R., A. E. Punt, and R. Hilborn. 2011. Spatial structure induced by marine reserves
784 shapes population responses to catastrophes in mathematical models. Ecological
785 applications 21:1399-1409.
786 McGilliard, C. R., A. E. Punt, R. Hilborn, and T. Essington. 2017. Modeling the impacts of two
787 age-related portfolio effects on recruitment variability with and without a marine reserve.
788 Ecological applications 27:1985-2000.
789 McKechnie, I., D. Lepofsky, M. L. Moss, V. L. Butler, T. J. Orchard, G. Coupland, F. Foster, M.
790 Caldwell, and K. Lertzman. 2014. Archaeological data provide alternative hypotheses on
791 Pacific herring (*Clupea pallasii*) distribution, abundance, and variability. Proceedings of
792 the National Academy of Sciences 111:E807-E816.
793 Melbourne, B. A., and P. Chesson. 2006. The scale transition: scaling up population dynamics
794 with field data. Ecology 87:1478-1488.
795 Merrick, R. L., and T. R. Loughlin. 1997. Foraging behavior of adult female and young-of-the-
796 year Steller sea lions in Alaskan waters. Canadian Journal of Zoology 75:776-786.
797 Mitamura, H., K. Uchida, Y. Miyamoto, N. Arai, T. Kakihara, T. Yokota, J. Okuyama, Y.
798 Kawabata, and T. Yasuda. 2009. Preliminary study on homing, site fidelity, and diel
799 movement of black rockfish *Sebastes inermis* measured by acoustic telemetry. Fisheries
800 Science 75:1133-1140.
801 Moser, M. L., M. S. Myers, J. E. West, S. M. O'Neill, and B. J. Burke. 2013. English sole
802 spawning migration and evidence for feeding site fidelity in Puget Sound, USA, with
803 implications for contaminant exposure. Northwest Science 87:317-325.
804 Nesbitt, H. K., and J. W. Moore. 2016. Species and population diversity in Pacific salmon
805 fisheries underpin indigenous food security. Journal of Applied Ecology 53:1489-1499.

806 Nielsen, J. K., P. N. Hooge, S. J. Taggart, and A. C. Seitz. 2014. Characterizing Pacific halibut
807 movement and habitat in a Marine Protected Area using net squared displacement
808 analysis methods. Marine Ecology Progress Series 517:229-250.
809 Nisbet, R. M., and W. Gurney. 1982. Modelling fluctuating populations. Wiley, New York.
810 Okamoto, D. K., M. R. Poe, T. B. Francis, A. E. Punt, P. S. Levin, A. O. Shelton, D. R.
811 Armitage, J. S. Cleary, S. C. Dressell, R. Jones, H. Kitka, L. C. Lee, A. D. MacCall, J. A.
812 McIsaac, S. Reifenstuhl, J. J. Silver, J. O. Schmidt, T. F. Thornton, R. Voss, and J.
813 Woodruff. 2019. Attending to spatial social–ecological sensitivities to improve trade-off
814 analysis in natural resource management. Fish and Fisheries.
815 Okamoto, D. K., R. J. Schmitt, and S. J. Holbrook. 2016. Stochastic density effects on adult fish
816 survival and implications for population fluctuations. Ecology letters 19:153-162.
817 Pearce, J. M., J. A. Reed, and P. L. Flint. 2005. Geographic variation in survival and migratory
818 tendency among North American Common Mergansers. Journal of Field Ornithology
819 76:109-118.
820 Peery, M. Z., S. H. Newman, C. D. Storlazzi, and S. R. Beissinger. 2009. Meeting reproductive
821 demands in a dynamic upwelling system: foraging strategies of a pursuit-diving seabird,
822 the marbled murrelet. The Condor 111:120-134.
823 Peterson, D. A., R. Hilborn, and L. Hauser. 2014. Local adaptation limits lifetime reproductive
824 success of dispersers in a wild salmon metapopulation. Nature communications 5.
825 Peterson, S. H., M. M. Lance, S. J. Jeffries, and A. Acevedo-Gutiérrez. 2012. Long distance
826 movements and disjunct spatial use of harbor seals (*Phoca vitulina*) in the inland waters
827 of the Pacific Northwest. PloS one 7:e39046.

828 Punt, A. E., D. K. Okamoto, A. D. MacCall, A. O. Shelton, D. R. Armitage, J. S. Cleary, I. P.
829 Davies, S. C. Dressel, T. B. Francis, and P. S. Levin. 2018. When are estimates of
830 spawning stock biomass for small pelagic fishes improved by taking spatial structure into
831 account? Fisheries research 206:65-78.
832 Rand, K. M., P. Munro, S. K. Neidetcher, and D. G. Nichol. 2014. Observations of seasonal
833 movement from a single tag release group of Pacific cod in the eastern Bering Sea.
834 Marine and Coastal Fisheries 6:287-296.
835 Ricker, W. 1958. Maximum sustained yields from fluctuating environments and mixed stocks.
836 Journal of the Fisheries Board of Canada 15:991-1006.
837 Rieman, B., and J. Dunham. 2000. Metapopulations and salmonids: a synthesis of life history
838 patterns and empirical observations. Ecology of Freshwater Fish 9:51-64.
839 Rogers, L. A., A. K. Salomon, B. Connors, and M. Krkošek. 2018. Collapse, tipping points, and
840 spatial demographic structure arising from the adopted migrant life history. The
841 American Naturalist 192:49-61.
842 Salomon, A., A. Quinlan, G. Pang, D. Okamoto, and L. Vazquez-Vera. 2019. Measuring social-
843 ecological resilience reveals opportunities for transforming environmental governance.
844 Ecology and Society 24.
845 Schindler, D. E., R. Hilborn, B. Chasco, C. P. Boatright, T. P. Quinn, L. A. Rogers, and M. S.
846 Webster. 2010. Population diversity and the portfolio effect in an exploited species.
847 Nature 465:609-612.
848 Schtickzelle, N., and T. P. Quinn. 2007. A metapopulation perspective for salmon and other
849 anadromous fish. Fish and Fisheries 8:297-314.

Secor, D. H., L. A. Kerr, and S. X. Cadrin. 2009. Connectivity effects on productivity, stability, and persistence in a herring metapopulation model. ICES Journal of Marine Science 66:1726-1732.

Seitz, A. C., T. Loher, B. L. Norcross, and J. L. Nielsen. 2011. Dispersal and behavior of Pacific halibut *Hippoglossus stenolepis* in the Bering Sea and Aleutian Islands region. Aquatic Biology 12:225-239.

Shelton, A., J. Samhouri, A. Stier, and P. Levin. 2014. Assessing trade-offs to inform ecosystem-based fisheries management of forage fish. Scientific Reports 4.

Shelton, A. O., and M. Mangel. 2011. Fluctuations of fish populations and the magnifying effects of fishing. Proceedings of the National Academy of Sciences 108:7075-7080.

Siple, M. C., and T. B. Francis. 2016. Population diversity in Pacific herring of the Puget Sound, USA. Oecologia 180:111-125.

Spies, I., P. D. Spencer, and A. E. Punt. 2015. Where do we draw the line? A simulation approach for evaluating management of marine fish stocks with isolation-by-distance stock structure. Canadian journal of fisheries and aquatic sciences 72:968-982.

Stan Development Team. 2016a. RStan: the R interface to Stan. Version 2.10.1. <http://mc-stan.org/rstan.html>

Stan Development Team. 2016b. Stan: A C++ library for probability and sampling. Version 2.12.0. <http://mc-stan.org>

Steneck, R., T. Hughes, J. Cinner, W. Adger, S. Arnold, F. Berkes, S. Boudreau, K. Brown, C. Folke, and L. Gunderson. 2011. Creation of a gilded trap by the high economic value of the Maine lobster fishery. Conservation biology 25:904-912.

872 Stephenson, R. L. 1999. Stock complexity in fisheries management: a perspective of emerging
873 issues related to population sub-units. Fisheries Research 43:247-249.
874 Stone, R. P., and C. E. O'Clair. 2001. Seasonal movements and distribution of Dungeness crabs
875 Cancer magister in a glacial southeastern Alaska estuary. Marine Ecology Progress Series
876 214:167-176.
877 Takashina, N., and A. Mougi. 2015. Maximum sustainable yields from a spatially-explicit
878 harvest model. Journal of Theoretical Biology 383:87-92.
879 Tanasichuk, R., A. Kristofferson, and D. Gillman. 1993. Comparison of some life history
880 characteristics of Pacific herring (*Clupea pallasi*) from the Canadian Pacific Ocean and
881 Beaufort Sea. Canadian Journal of Fisheries and Aquatic Sciences 50:964-971.
882 Thornton, T. F., and H. Kitka. 2015. An indigenous model of a contested Pacific Herring fishery
883 in Sitka, Alaska. International Journal of Applied Geospatial Research 6:94-117.
884 Tolimieri, N., K. Andrews, G. Williams, S. Katz, and P. Levin. 2009. Home range size and
885 patterns of space use by lingcod, copper rockfish and quillback rockfish in relation to diel
886 and tidal cycles. Marine Ecology Progress Series 380:229-243.
887 von der Porten, S., J. Corntassel, and D. Mucina. 2019. Indigenous nationhood and herring
888 governance: strategies for the reassertion of Indigenous authority and inter-Indigenous
889 solidarity regarding marine resources. AlterNative: An International Journal of
890 Indigenous Peoples:1177180118823560.
891 von der Porten, S., D. Lepofsky, D. McGregor, and J. Silver. 2016. Recommendations for marine
892 herring policy change in Canada: Aligning with Indigenous legal and inherent rights.
893 Marine Policy 74:68-76.

894 Wang, S., and M. Loreau. 2014. Ecosystem stability in space: α, β and γ variability. Ecology
895 letters 17:891-901.
896 Ward, E. J., P. S. Levin, M. M. Lance, S. J. Jeffries, and A. Acevedo-Gutiérrez. 2012. Integrating
897 diet and movement data to identify hot spots of predation risk and areas of conservation
898 concern for endangered species. Conservation Letters 5:37-47.
899 Wespestad, V. G., K. Thorsen, and S. Mizroch. 1983. Movement of sablefish, *Anoplopoma*
900 *fimbria*, in the northeastern Pacific Ocean as determined by tagging experiments (1971-
901 80). Fishery Bulletin 81:415-420.
902 Young, O. R. 2002. The institutional dimensions of environmental change: fit, interplay, and
903 scale. MIT press.
904

905 Table 1: Equations used in Model 2 (Pacific herring case-study: spatial variability in biomass and

906 catch)

Eq	**Description**	**Equation**
Eq. 8	Expected pre-spawn biomass	$\hat{b}^{+}_{t+1,l} = \exp\left(\alpha_l + (1-\beta_l)\ln(b_{t-1,l})\right) + \lambda_l b_{t,l}$
Eq. 9	Estimated log-biomass	$\ln \boldsymbol{b}^{+}_{t} = \ln(e^{\ln \boldsymbol{b_t}} + \boldsymbol{h}_t) \sim \text{MVN}(\ln \widehat{\boldsymbol{b}}^{+}_{t}, \text{diag}(\boldsymbol{\sigma})\Omega)$
Eq. 10	Objective function	$\ell = \sum_{t=1}^{T}\sum_{l=1}^{L} \frac{\left(\ln(\text{obs}[b_{t,l}]) - (\ln b_{t,l} + \ln q)\right)^2}{(2\sigma^2_{obs})} - \ln(\lvert \text{d} \rvert)$
Eq. 11	Jacobian adjustment for change of variables in Eq. 10	$\text{d} = \frac{\partial}{\partial \ln b_{t,l}} \ln(e^{\ln b_{t,l}} + h_{t,l}) = \frac{b_{t,l}}{b_{t,l} + h_{t,l}}$
Symbol	**Description**	**Prior or Data Source**
α_l	Site-specific Gompertz productivity	$[\alpha_l \quad \text{logit}(\beta_l) \quad \text{logit}(\lambda_l)]' \sim \text{MVN}(\boldsymbol{\Theta}, \boldsymbol{\sigma}_\Theta \Omega_\Theta)$;
β_l	Site-specific Gompertz compensation	
λ_l	Site-specific aggregate mortality & somatic growth	
Θ	Mean vector for $\alpha, \text{logit}(\beta)$, and $\text{logit}(\lambda)$	$\boldsymbol{\Theta} \sim \text{MVN}(0, \text{diag}(1.5)\Omega_{\bar{\Theta}})$;
σ_{Θ_l}	Among site variances in $\alpha, \text{logit}(\beta)$, and $\text{logit}(\lambda)$	$\sigma_{\Theta_l} \sim$ half-cauchy(0, 2.5)
Ω	Process error spatial corr. matrix	LKJ prior (Lewandowski et al. 2009): scale = 2
Ω_Θ	parameter corr. matrix	
$\Omega_{\bar{\Theta}}$	mean parameter corr. matrix	
$\boldsymbol{\sigma}$	Vector of site-specific lognormal process variances	$\sigma_l \sim \text{normal}(\sigma_\mu, 0.15)$; $\sigma_\mu \sim \text{normal}(0, 0.15)$
σ_{obs}	Lognormal obs. error	$\sigma_{obs} \sim$ half-cauchy(0, 2.5)
$\ln q$	Survey bias (egg "catchability")	$\ln q \sim \text{normal}(0, 0.05)$ (Martell et al. 2012)
$\text{obs}[b_{t,l}]$	Input Data	observed spawning biomass at time t at location l
$h_{t,l}$	Input Data	harvest at time t at location l

907 Table 2: Equations used in Model 3 (Solutions for spatial scale mismatches in fished herring

908 metapopulations). See Table 3 for parameter values and definitions.

909

Eq	Description	Equation
Eq. 12	Recruits (age 2) prior to movement	$n^{++}_{a=2,l,t+2} = \text{eggs}_{l,t} \exp\left[\epsilon_{l,t} - \frac{{\sigma_r}^2}{2}\right] / (\alpha + \beta \text{eggs}_{l,t})$
Eq. 13	Total eggs lain	$\text{eggs}_{l,t} = \sum_{a=2}^{10} \text{m}_a \text{f}_a [0.5 n_{a,l,t}]$
Eq. 14	Environmental recruitment stochasticity	$\boldsymbol{\epsilon_t} = \phi \boldsymbol{\epsilon_t} + \text{MVN}(0, {\sigma_r}^2 [1 - \phi^2] \boldsymbol{\Omega}_r)$
Eq. 15	Spatial correlation in recruitment stochasticity	$\rho_{i,j} = \exp\left(-\frac{2\sin^2\pi \left\| dist_{i \to j} \right\|}{\eta^2}\right)$
Eq. 16	Pre-harvest abundance	$n^{++}_{a,l,t+1} = \begin{cases} \lambda_t \, n_{a-1,l,t} & 2 < a < 10 \\ \lambda_t \, n_{a-1,l,t} + \lambda_t \, n_{a,l,t} & a = 10 \text{ (plus group)} \end{cases}$
Eq. 17	Post-migration abundance	$\boldsymbol{N}^{+}_{t} = \boldsymbol{N}^{++}_{t} \boldsymbol{S}; \;\; S_{i,j} = \text{P}(i \to j)$
Eq. 18	Recruit or Adult migration by distance function	$\text{P}(i \to j) = \exp\left(-\frac{2\sin^2\pi \left\| dist_{i \to j} \right\|}{\gamma^2}\right) \sum_{j=1}^{N} \exp\left(-\frac{2\sin^2\pi \left\| dist_{i \to j} \right\|}{\gamma^2}\right)^{-1}$
Eq. 19	Quota	$\widehat{Q}_{t+l} = \begin{cases} min\left(H_{Target} * \hat{B}_{forecast,t}, \hat{B}_{forecast,t} - L_{crit} * \hat{B}_{0,t}\right) & \text{if } \widehat{B}_{forecast,t} \geq L_{crit} * \hat{B}_{0,t} \\ 0 & \text{otherwise} \end{cases}$
Eq. 20	Post-harvest abundance at age in year t	$n_{a,l,t} = (1 - \text{m}_a) n^{+}_{a,l,t} - \text{m}_a n^{+}_{a,l,t} e^{-F_{t,l}}; \;\; F_{t,l} = \ln h_{t,l} \,/ \sum_{a=2}^{10} \text{w}_a \text{m}_a \, n^{+}_{a,l,t}$
Eq. 21	Biomass at location *l* in year t	$B_{l,t} = \sum_{a=2}^{10} \text{w}_a \text{m}_a \, n^{+}_{a,l,t}$

910

911 Table 3: List of key parameters and state-variables in Model 3 with definitions, values and
912 citations. Note that equilibrium considerations are generated by simulating with no harvest and
913 no stochasticity (σ_r = 0, cv in λ_t = 0, and harvest = 0). Selectivity-at-age in all cases is equal to
914 maturity-at-age.

Parameter	Description	Value(s)	Source
$\boldsymbol{\alpha, \beta}$	Beverton-Holt stock-recruit parameters	583.43, 2.089 x 10^{-8}	1
$\boldsymbol{\phi}$	1st order partial autocorrelation	0.6	Chosen
m_a	Maturity-at-age (=Selectivity-at-age)	Age 1 = 0, Age 2= 0.2, Age 3=0.9, Age 4 + = 1	2
w_a	Weight-at-age	$4.5x10^{-6}$ [27(1-Exp(-0.48*age)]$^{3.127}$	3
f_a	Fecundity-at-age	$\exp(4.69)(1000w_a)^{1.13}$	3
λ_t	Annual pre-harvest survival rate	Beta-binomial: mean = 0.6, cv= 0.2	Derived from 1
$\boldsymbol{\sigma_r}$	Stock-scale standard deviation of rec-devs	0.8	1
η	Scale parameter regulating distance decay in rec-dev spatial covariance	Numerically tuned to achieve desired spatial correlations	Chosen
L_{crit}	Lower biomass threshold for fishing closure relative to $\hat{B}_0$	0.25	1
$\overline{P}(i \rightarrow j)$	Mean migration probability	0.01 to 0.8	Chosen
$\bar{\rho}_{i,j}$	Spatial synchrony in recruitment	0.15 to 0.85	Chosen
State Variable	**Description**		
$n^{++}_{a,l,t}$	Abundance at age *a* in time *t* at location *l* prior to movement and harvest (Eq. 16)		
$n^{+}_{a,l,t}$	Abundance after movement and prior to harvest (Eq. 17)		
$F_{t,l}$	Fishing mortality of susceptible fish at time *t* at location *l* after movement and natural mortality (Eq. 20)		

915 1: (Department of Fisheries and Oceans 2015)

916 2: (Martell et al. 2011)

917 3: (Tanasichuk et al. 1993)

Table 4: Home-range categories of different Pacific herring predator groups. Details of sources and home-ranges are provided in the DataS1:Appendix S4.

Home-Range Category	Home-Range Description	Herring Predator Groups
Localized	single subpopulation *(< 10 km radius)*	Indigenous fishers**, Seabirds*, Flatfishes*, Crustaceans*, Urchins, Cucumbers, Reef Fishes, Rockfishes
Centralized	multiple subpopulations *(~10-40 km-radius)*	Indigenous fishers**, Seabirds*, Flatfishes*, Crustaceans*, Gadiforms*, Salmonids**, Halibut**, Harbor Seals
Transient	full stock or greater	Seine & Gillnet Fishers, Cetaceans, Sea Lions, Seabirds*, Gadiforms*, Salmonids**, Halibut**

*Varies by species, ** Varies by migration phase, location or individual

924 List of Figures:

925 Figure 1: Effect of elevating harvest mortality rate on asynchrony related spatial variability in the
926 metapopulation from Model 1. **(a)** Spatial variation increases as a function of total mortality for
927 different levels of spatial synchrony in recruitment productivity. Here migration is held at 0.25
928 and log-scale recruitment variability (σ_R) is 0.7 (i.e. CV = 0.8). Note spatial variation is a result
929 of the discrepancy in population versus metapopulation temporal variation in panel
930 (b); **(b)** Temporal variability (squared coefficient of variation) of the population and
931 metapopulation. The arrows illustrate spatial variability as the difference between
932 surfaces. **(c)** Measures of local population predictability (measured by first order within
933 population autocorrelation, thick black line), among population coupling (measured by among
934 population correlations, thin black line), and local environmental sensitivity (measured by the
935 response at the population level to a unit environmental impulse affecting recruitment
936 productivity, red line).

937

938 Figure 2: **(a)** Map of major Pacific Herring spawning substocks ("Sections" - denoted by
939 different symbols) as defined by Canada's Federal Fisheries Agency in the Central Coast of
940 British Columbia. Indigenous communities noted with *. **(b)** Trends for the six main
941 supopulations (substocks - thin colored lines & points) and the metapopulation (stock) mean
942 (thick blue line). Trends were estimated using multivariate hierarchical Bayesian state-space
943 model integrating spawn surveys and catch information (model 2). Individual plots for each
944 substock are shown, along with catch, spawn observations, and 95% posterior credible intervals
945 in Appendix S2. **(c)** Temporal coefficients of variation estimated from the Bayesian state-space
946 mode over 25 years for each substock, the mean of each substock CV (large black symbol), the

947 regional stock coefficient of variation (blue point), and the spatial variability (black point with
948 error bar) which is the standardized variance of the system after accounting for the variance of
949 the stock and the variance of the substock means. Error bars are 95% credibility intervals. (d)
950 Trends in annual harvest rate for 2 of the 6 local substocks (Higgins and Lower Spiller) with
951 points, 95% credibility intervals and the mean for the aggregate stock (thick blue line). For full
952 results see Appendix S2. The dotted line represents the target harvest rate of 20%.
953
954 Figure 3: Mean risk of collapse (%) at metapopulation and subpopulation scales for different
955 harvest rates and spatial harvest allocation strategies under varying spatial scenarios. Results are
956 derived from simulation-based risk analysis of hypothetical Pacific herring fisheries. Axes
957 present simulations with different levels of annual migration and spatial synchrony in
958 recruitment productivity, columns represent different harvest strategies and rows represent the
959 spatial scales of inference. Risk of collapse is the probability of falling below 20% of unfished
960 equilibrium (i.e. the dotted lines in Fig. 4 a-c); at the subpopulation scale, risk is measured as the
961 mean probability of collapse for each population. *Optimized allocation* harvests proportionally
962 more from subpopulations with higher biomass; *Proportional allocation* removes the same
963 proportion of biomass from each subpopulation. Annual migration is the mean percent of each
964 subpopulation that emigrates each year and spatial synchrony is the mean pairwise correlation in
965 recruitment productivity. For full results see Appendix S3: Fig. S2. Note that the allocation
966 strategies produce equivalent average yields (Figure 3c vs. 3e and 3g vs. 3i; see Appendix S3:
967 Fig. S3 for yield comparisons). For an illustration of how alternative strategies affect the mean
968 duration of collapses, see Appendix S3: Fig. S4.
969

970 Figure 4: **(a-c)** Example simulations (a single simulation run) showing spatial variation in
971 biomass measured at the subpopulation level (colored lines) or metapopulation mean (thick blue)
972 for **(a)** an unexploited metapopulation, **(b)** a 20% target harvest allocated proportional to
973 spawning biomass in space, or **(c)** a 20% target harvest allocated optimally in space according to
974 the ideal free distribution (see Appendix S3: Fig. S4 for summaries across runs). B_0 =
975 deterministic biomass in the absence of fishing, dotted line = lower conservation threshold of
976 20% of B_0. **(d)** change in spatial variation for different harvest rates and spatial harvest allocation
977 across different spatial parameter scenarios for migration rates and spatial synchrony. Each point
978 represents the spatial variance from 100 runs from a single 52-year simulation using a unique
979 migration-synchrony parameter combination.
980

Figure 1

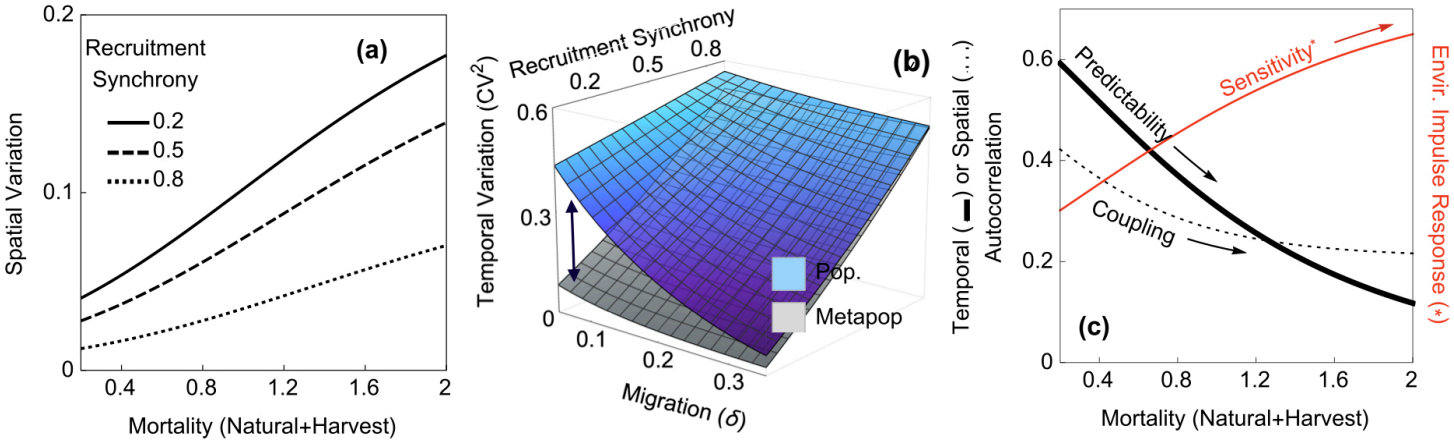

Figure 2

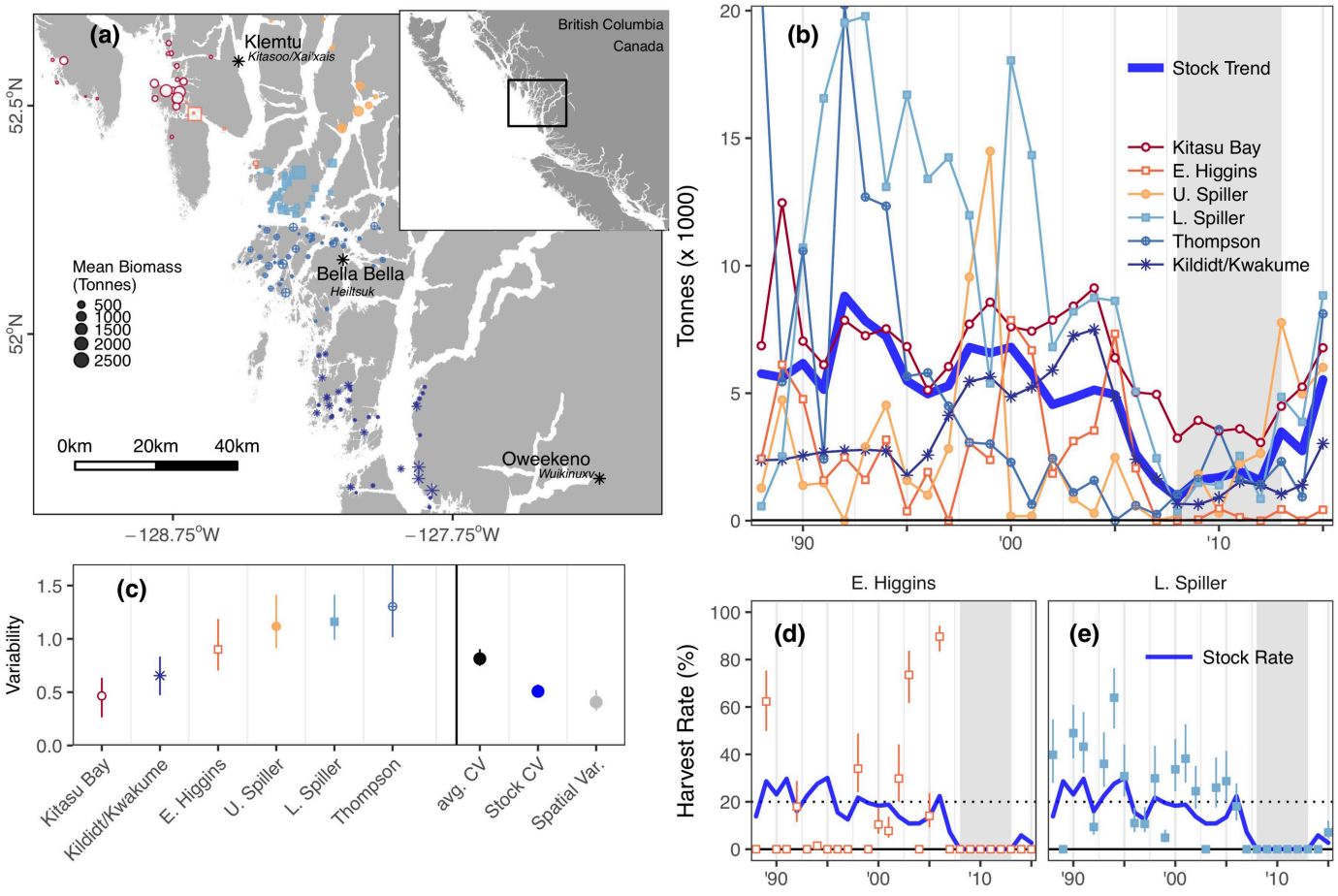

Figure 3

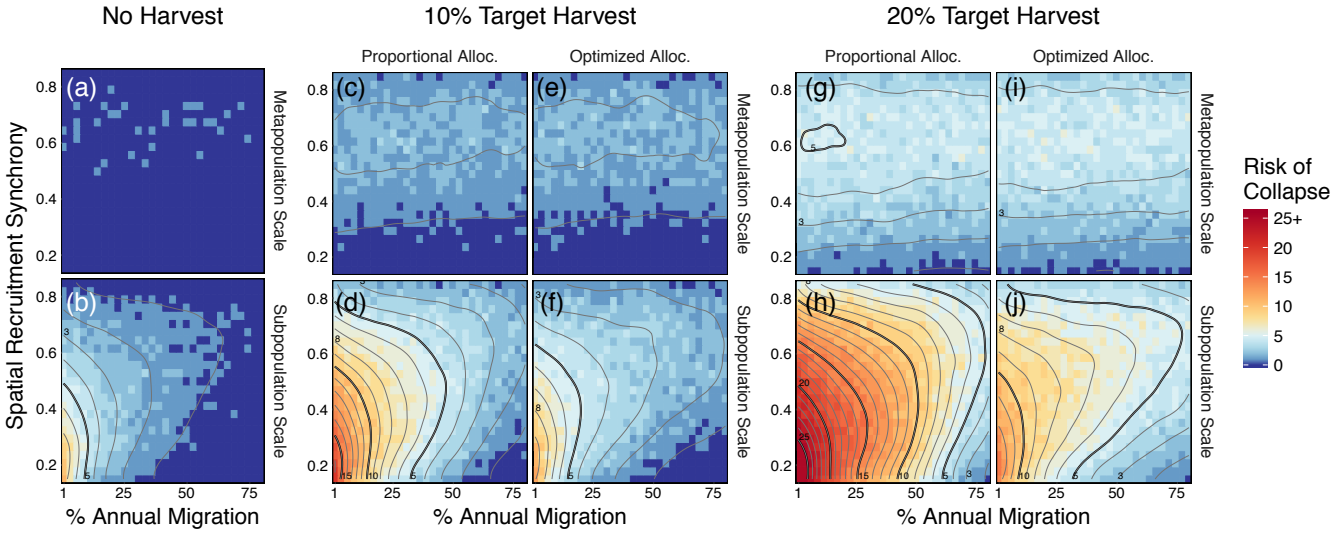

Figure 4